Effects of γ-ray irradiation on ferroelectric properties of Pr and Mn co-substituted $BiFeO_3$ thin films

Zheng Wen,[1,2] Di Wu,[1,a)] Jiating Zhu,[3] and Aidong Li[1]

[1]*National Laboratory of Solid State Microstructures, Nanjing University, Nanjing 210093, China and Department of Materials Science and Engineering, College of Engineering and Applied Sciences, Nanjing University, Nanjing 210093, China*

[2]*College of Physical Science, Qingdao University, Qingdao 266071, China*

[3]*Institute for Application of Atomic Energy, Jiangsu Academy of Agriculture Sciences, Nanjing 210014, China*

Abstract

γ-ray irradiation effects on ferroelectric properties of $(Bi_{0.85}Pr_{0.15})(Fe_{0.95}Mn_{0.05})O_3$ (BPFMO) thin films are investigated by pizeoresponse force microscopy and polarization-voltage hysteresis measurements. The irradiated BPFMO thin-film capacitors show reduced polarizations and imprinted hysteresis loops. The loss of nonvolatile polarization increases with the decrease of polarization values prior to the irradiation and the imprint of hysteresis loops depends on the direction of polarization. These are discussed in terms of separation of γ-ray-excited electron-hole pairs by the depolarization field and subsequent charge trapping and aggregation on charged domain walls in BPFMO thin films.

[a)]Author to whom correspondence should be addressed. Electronic mail: diwu@nju.edu.cn

Among all known perovskite oxides, $BiFeO_3$ (BFO) is the only room temperature single-phase multiferroic to date.[1] Large spontaneous polarizations, as high as ~ 100 μC/cm^2, with coupling between electric and magnetic orders have been reported in thin-film BFO, which demonstrates great application potentials of BFO in ferroelectric random access memories and electrically controlled magnetic devices.[2-4] Recently, Jiang and co-workers reported resistive switching behaviors in Pt/BFO/$SrRuO_3$ heterostructures by modulating interfacial Schottky-like barriers with polarization reversal.[5,6] In ultrathin BFO films that allow quantum tunneling, tunneling electroresistance and memristive characteristics have been achieved in Pt/Co/BFO/(Ca,Ce)MnO_3 junctions through controlling the barrier profile by gradual modulating the effective polarization.[7] Furthermore, non-volatile switching between four resistance states has also been reported in all-oxide (La,Sr)MnO_3/BFO/(La,Sr)MnO_3 multiferroic tunnel junctions.[8] Unusual photovoltaic properties with open-circuit voltages higher than the band-gap of BFO are observed in BFO thin films with ordered stripe domain arrays.[9,10] Employing the photovoltaic effect, Guo *et al*. recently demonstrated an interesting prototype memory based on Fe/BFO/(La,Sr)MnO_3 heterostructures with non-destructive readout through monitoring the photo-generated voltages that are dependent on the polarization directions.[11]

Functionalities of these devices depend on the effective polarization and domain switching in BFO thin films. It is well known that high energy γ-ray and synchrotron X-ray irradiations may result in polarization loss, imprint and possible retention failure in ferroelectric thin films, as reported previously in Pb(Zr,Ti)O_3, $PbTiO_3$ and $SrBi_2Ta_2O_9$ thin-film devices.[12-16] For

ferroelectric thin films in military and space applications, irradiation induced performance deterioration may be more severe due to the higher possibility to be exposed to high energy irradiations. However, there is yet no report on high energy irradiation effects on ferroelectric properties of BFO-based thin films, although the irradiation resistance is important to the device reliability. In this work, effects of γ-ray irradiation on ferroelectric properties of $(Bi_{0.85}Pr_{0.15})(Fe_{0.95}Mn_{0.05})O_3$ (BPFMO) thin films are studied. Reduction in nonvolatile polarizations and shift of hysteresis loops are observed in irradiated BPFMO thin-film capacitors. Possible origins responsible for these behaviors are discussed.

BPFMO thin films were prepared on $Pt/TiO_2/SiO_2/Si$ substrates by chemical solution deposition using spin-coating, as reported previously.[17] Each layer of the BPFMO was baked at 300 ^{0}C, pyrolyzed at 400 ^{0}C for 10 min in O_2, and then annealed at 525 ^{0}C for 3 min in N_2. The spin-coating and heat treatment steps were repeated for several times to obtain the desired film thickness. Finally, the films were annealed at 525 ^{0}C for 30 minutes in N_2. X-ray diffraction (XRD), performed using a Rigaku Ultima-III diffractrometer with Cu Kα radiation, was used to characterize the structure of BPFMO thin films. Cross-sectional morphology of the $BPFMO/Pt/TiO_2/SiO_2/Si$ stack was acquired using a FEI Quanta 200 scanning electron microscope (SEM). The surface topology and domain structure of BPFMO thin films were characterized using an Asylum Research Cypher scanning probe microscope. The atomic force microscopy (AFM) images were recorded in a tapping mode. Pizeoresponse force microscopy (PFM) was conducted in a single-frequency mode using Olympus AC240TM Pt/Ti-coated silicon

cantilevers with a contact resonant frequency about 300 kHz. The phase images were acquired at a driving amplitude of 3 V, well below the coercive voltage (V_c) of BPFMO, and a frequency of 20 kHz, far from the resonant frequency, to eliminate the possible position-dependent phase shift due to the surface roughness. Pt top electrodes of 100 μm in diameter were sputter-deposited with a shadow mask. A commercial ferroelectric tester (Precision Multiferroic, Radiant Technologies) was used to acquire the Positive-Up-Negative-Down (PUND) polarization data and the polarization-voltage hysteresis loops of Pt/BPFMO/Pt thin-film capacitors at 10 kHz. The BPFMO thin films were subjected to 1.33-MeV γ-ray from a ^{60}Co source for 24 hours with a total dose of 5.0 Mrad (SI).

The XRD pattern, shown in Fig. 1(a), indicates that the BPFMO film is phase-pure and polycrystalline on Pt/TiO_2/SiO_2/Si substrates.[18] The BPFMO film is about 500 nm in thickness and exhibits a clear interface with the Pt bottom electrode (Fig. 1(b)). The film is composed of closely-packed spherical grains of about 50 nm in size. The surface root-mean-square roughness is about 1.54 nm over an area of 1×1 μm^2, as measured from the AFM image shown in Fig. 1(c).

Fig. 2(a) shows polarization-voltage hysteresis loops of Pt/BPFMO/Pt thin-film capacitors at various voltages. Remanent polarization (P_r) and coercive voltage are plotted in Fig. 2(b) as functions of the applied voltage. Both P_r and V_c increase rapidly at the range of 5-15 V and saturate above 15 V. At the above-saturation voltage of 25 V, P_r and V_c of the Pt/BPFMO/Pt are about 80 μC/cm^2 and 9 V, respectively. These values are comparable to those reported in the literature.[1,2]

PFM out-of-plane phase images of domains written in fresh and irradiated BPFMO thin films are shown in Fig. 3(a) and (b). By scanning the conductive-tip over an area of 3×3 μm^2 with a +20 V bias (white square in Fig. 3(a)) and then the central 1.5×1.5 μm^2 with a -20 V bias (orange square in Fig. 3(a)), the BPFMO thin films can be fully polarized downward (dark cyan) and upward (bright) with a phase contrast about 180^0. The tip-written domain structures in both fresh and irradiated BPFMO films were checked after a 12-hour retention time, as shown in Fig. 3(c) and (d). It is observed that the domain structure written in the fresh BPFMO does not change significantly, indicating good retention of polarization. However, in the irradiated BPFMO, clear backswitching of the downward domain is observed after 12 hours, as shown in Fig. 3(d). This indicates the upward polarization (bright) becomes more energetically favorable in the irradiated BPFMO films.

The preferred upward polarization can also be seen from the irradiation-induced domain structure change in the un-written area. As shown in Fig. 3(a), the un-written area in the fresh film exhibits a multi-domain structure with slightly more upward nano-domains. However, after irradiation, this un-written area shows a predominantly bright contrast (Fig. 3(b)), indicating a preferred upward polarization. The appearance of preferred polarization direction implies the formation of an extra field in the film, which stabilizes the upward domains.

Nonvolatile polarization (P_{nv}) values[19] of the fresh and the irradiated Pt/BPFMO/Pt thin-film capacitors are evaluated by PUND measurements as a function of pulse amplitude from 13 V up to 25 V. The measurements are shown schematically in the inset of Fig. 4(a). P_{nv} of fresh

Pt/BPFMO/Pt capacitors was measured first. The PUND pulses (blue) leave the capacitor polarized upward. The capacitors are then subjected to γ-ray irradiation. After the irradiation of prescribed dosage, P_{nv} of the capacitors is measured again using PUND pulses (red). Reduction of P_{nv} is observed after γ-ray irradiation. And the irradiation-induced P_{nv} loss increases with the decrease of poling voltage before irradiation, as plotted in Fig. 4(b).

The loss of P_{nv} can be understood in terms of domain pinning that is essential in polarization fatigue of BFO-based thin films due to repetitive switching.[20,21] Non-180^0 domain walls may exist in polycrystalline BPFMO thin films, as depicted schematically in Fig. 4(e).[21] In a certain domain a depolarization field (E_d) develops pointing against the polarization as a result of incomplete screening of the polarization charges. When the BPFMO thin films are subjected to γ-ray irradiation, electron-hole pairs can be excited inside the film.[22] These electron-hole pairs are separated and swept out towards domain walls by the local E_d. The electrons and holes trapped at charged non-180^0 domain walls help to screen the polarization charges and stabilize the domain structure by lowering the electrostatic energy. The aggregation of space charges on the domain walls may block domain switching, resulting in reduced polarizations observed in Fig. 4(a). The density of domain walls in BPFMO increases with decreasing poling voltage due to partial switching and domain misalignment under sub-saturation voltages. The increase of domain wall density increases the possibility of charge trapping and results in larger P_{nv} loss in irradiated Pt/BPFMO/Pt capacitors, as shown in Fig. 4(b).

In fact, the aggregation of γ-ray-excited charges on charged domain walls produces an extra

electric field, E_i in Fig. 4(e), in parallel with the polarization. This irradiation-induced extra field stabilizes the polarization state prior to irradiation and results in asymmetric domain switching, which in turn gives rise to retention and imprint issues in irradiated BPFMO. The polarization in as-deposited BPFMO thin films is pointed preferentially upward. Therefore, an upward E_i develops in the irradiated BPFMO. After the PFM writing, this upward E_i may facilitate backswitching of downward domains during the 12-hour retention, as observed in Fig. 3(d).

Fig. 4(c) and (d) demonstrate imprint effect in the irradiated Pt/BPFMO/Pt capacitors due to the existence of E_i and the accompanied asymmetric domain switching. The imprint depends on the polarization prior to irradiation. The $-P_r$/irradiation combination results in a positive shift of the hysteresis loop along the horizontal axis, while the $+P_r$/irradiation procedure shifts the hysteresis loop toward negative voltage. Typical hysteresis loops of fresh and irradiated Pt/BPFMO/Pt capacitors, polarized upward or downward prior to irradiation, are shown in Fig. 4(d) for clarity. The value of hysteresis shift[23] increases with decreasing poling voltage. For example, the lateral negative shift of hysteresis loop after $+P_r$/irradiation is 1.52 V in capacitors polarized by an above-saturation 25 V pulse, but increases to 1.85 V in capacitors polarized by a sub-saturation 13 V pulse. This can be ascribed to the increased density of domain walls in partially polarized BPFMO, where more trapping sites are available for γ-ray-excited space charges, leading to the increased E_i after irradiation.

As shown in Fig. 5, the γ-ray-induced P_{nv} loss can be completely rejuvenated by subjecting the irradiated Pt/BPFMO/Pt capacitor to 10^6 cycles of saturation bipolar pulses of 25 V. This is

attributed to the field-assisted domain wall unpinning as observed previously in fatigued BPFMO thin films.[22] The excited space charges conglomerated on domain walls can be dispersed by the external field that is strong enough to overcome the Coulomb interaction. The pinned domains are then set free and thus the reduced polarization is restored. In accompany with the polarization rejuvenation, the irradiation-induced imprint is also alleviated as a result of the redistribution of space charges after bipolar pulse cycling, which weakens the E_i.

In summary, γ-ray irradiation effects on ferroelectric properties of Pt/BPFMO/Pt thin-film capacitors are investigated. The irradiated Pt/BPFMO/Pt capacitors show reduced polarizations and the loss of polarization is found to increase with the decrease of polarization values prior to γ-ray irradiation. Imprinted hysteresis loops are observed in irradiated Pt/BPFMO/Pt capacitors. The direction of imprint and the shift of hysteresis loops also depends on the polarization prior to irradiation. These phenomena originate from separation of γ-ray-excited electron-hole pairs driven by the internal field in BPFMO films and subsequent charge trapping and aggregation on charged domain walls, which gives rise to an extra field E_i to stabilize the polarization prior to irradiation. Both reduced P_{nv} and imprinted hysteresis loops can be rejuvenated simply by repetitive bipolar switching with saturation voltages. According to previous results reported in Pt/$SrBi_2Ta_2O_9$/Pt capacitors, strongly distorted hysteresis loops with P_{nv} loss as high as 40% and lateral shifts up to 50% are observed after synchrotron X-ray and γ-ray irradiations.[15,16] In Pt/BPFMO/Pt capacitors, the reduction of P_{nv} is only about 10% and the shift of hysteresis loop is less than 25% of the values in fresh BPFMO capacitors. These indicate a better resistance

against high energy irradiations in BPFMO and suggest its application in circumstances with irradiations.

This work was jointly sponsored by State Key Program for Basic Research of China (2009CB929503), Natural Science Foundation of China (91022001 and 51222206), Natural Science Foundation of Jiangsu Province (BK2012016) and Doctoral Foundation of Ministry of Education of China (20110091110013).

Reference:

[1]G. Catalan and J. F. Scott, Adv. Mater. **21**, 2463 (2009).

[2]J. Wang, J. B. Neaton, H. Zheng, V. Nagarajan, S. B. Ogale, B. Liu, D. Viehland, V. Vaithyanathan, D. G. Schlom, U. V. Waghmare, N. A. Spaldin, K. M. Rabe, M. Wuttig, and R. Ramesh, Science **299**, 1719 (2003).

[3]W. Eerenstein, N. D. Mathur, and J. F. Scott, Nature **442**, 759 (2006).

[4]T. Zhao, A. Scholl, F. Zavaliche, K. Lee, M. Barry, A. Doran, M. P. Cruz, Y. H. Chu, C. Ederer, N. A. Spaldin, R. R. Das, D. M. Kim, S. H. Baek, C. B. Eom, and R. Ramesh, Nat. Mater. **5**, 823 (2006).

[5]A. Q. Jiang, C. Wang, K. J. Jin, X. B. Liu, J. F. Scott, C. S. Hwang, T. A. Tang, H. B. Lu, and G. Z. Yang, Adv. Mater. **23**, 1277 (2011).

[6]C. Wang, K. J. Jin, Z. T. Xu, L. Wang, C. Ge, H. B. Lu, H. Z. Guo, M. He, and G. Z. Yang, Appl. Phys. Lett. **98**, 192901 (2011).

[7]H. Yamada, V. Garcia, S. Fusil, S. Boyn, M. Marinova, A. Gloter, S. Xavier, J. Grollier, E. Jacquet, C. Carrétéro, C. Deranlot, M. Bibes, and A. Barthélémy, ACS Nano DOI: 10.1021/nn401378t (2013).

[8]M. Hambe, A. Petraru, N. A. Pertsev, P. Munroe, V. Nagarajan, and H. Kohlstedt, Adv. Funct. Mater. **20**, 2436 (2010).

[9]S. Y. Yang, J. Seidel, S. J. Byrnes, P. Shafer, C. H. Yang, M. D. Rossell, P. Yu, Y. H. Chu, J. F. Scott, J. W. Ager. III, L. W. Martin and R. Ramesh, Nat. Nanotech. **5**, 143 (2010).

[10]M. Alexe, Nano Lett. **12**, 2193 (2012).

[11]R. Guo, L. You, Y. Zhou, Z. S. Lim, X. Zou, L. Chen, R. Ramesh, and J. Wang, Nat. Commun. (accepted for publication).

[12]J. F. Scott, C. A. Araujo, H. B. Meadows, L. D. McMillan, A. Shawabkeh, J. Appl. Phys. **66**, 1444 (1989).

[13]J. R. Schwank, R. D. Nasby, S. L. Miller, M. S. Rodgers, P. V. Dressendorfer, IEEE Trans. Nucl. Sci. **37**, 1703 (1990).

[14]A. Gruverman, B. J. Rodriguez, R. J. Nemanich, and A. I. Kingon, J. Appl. Phys. **92**, 2734 (2002).

[15]D. Wu, A. D. Li, H. Q. Ling, T. Yu, Z. G. Liu, and N. B. Ming, Appl. Phys. A **73**, 255 (2001).

[16]N. Menou, A. M. Castagnos, Ch. Muller, D. Goguenheim, L. Goux, D. J. Wouters, J. L. Hodeau, E. Dooryhee, and R. Barrett, J. Appl. Phys. **97**, 044106 (2005).

[17]Z. Wen, X. Shen, J. Wu, D. Wu, A. Li, B. Yang, Z. Wang, H. Chen, and J. Wang, Appl. Phys. Lett. **96**, 202904 (2010).

[18]I. Sosnowska, R. Przenioslo, P. Fischer, V. A. Murashov, J. Magn. Magn. Mater. 160, **384** (1996).

[19]Nonvolatile polarization P_{nv} is defined as the difference between the switched (P*) and non-switched polarization (P^), as shown in the inset of Fig. 4(a).

[20]S. H. Baek, C. M. Folkman, J. W. Park, S. Lee, C. W. Bark, T. Tybell, and C. B. Eom, Adv. Mater. **23**, 1621 (2011).

[21]Z. Wen, Y. Lv, D. Wu, and A. Li, Appl. Phys. Lett. **99**, 012903 (2011).

[22]F. H. Attix and W. C. Roesch, *Radiation Dosimetry* (Academic, New York, London, 1968) pp. 99-111.

[23]The irradiation-induced V_c shift is defined as the lateral shift of irradiated hysteresis loop with respect to the fresh loop, that is, $\left[\frac{(+V_c)+(-V_c)}{2}\right]_{irradiated} - \left[\frac{(+V_c)+(-V_c)}{2}\right]_{fresh}$.

Figure Captions:

FIG. 1. XRD pattern (a), cross-sectional SEM image (b), and surface AFM image (c) of BPFMO thin films deposited on Pt/TiO_2/SiO_2/Si substrates.

FIG. 2. (a) Polarization-voltage hysteresis loops of Pt/BPFMO/Pt thin-film capacitors under various voltages and (b) remanent polarizations and coercive voltages as functions of applied voltage.

FIG. 3. PFM out-of-plane phase images over 4×4 μm^2 for fresh (a, c) and irradiated (b, d) BPFMO thin films recorded as-written (a, b) and after 12-hour retention (c, d).

FIG. 4. (a) P_{nv} of fresh and irradiated Pt/BPFMO/Pt thin-film capacitors and (b) the loss of P_{nv} after γ-ray irradiation as functions of voltage. (c) Polarization direction dependent V_c shift as functions of voltage. Corresponding hysteresis loops are shown in (d). (e) Schematic drawings to illustrate the domain pinning and the formation of internal field in Pt/BPFMO/Pt after γ-ray irradiation.

FIG. 5. Hysteresis loops of the fresh, irradiated and rejuvenated Pt/BPFMO/Pt capacitors.

Figures:

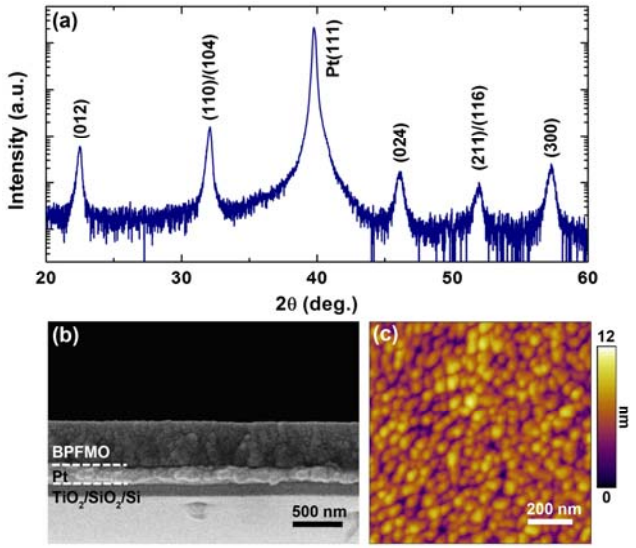

FIG. 1

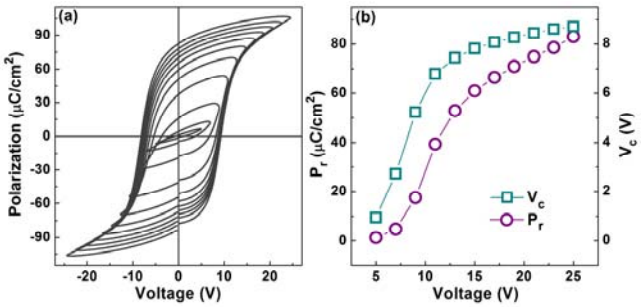

FIG. 2

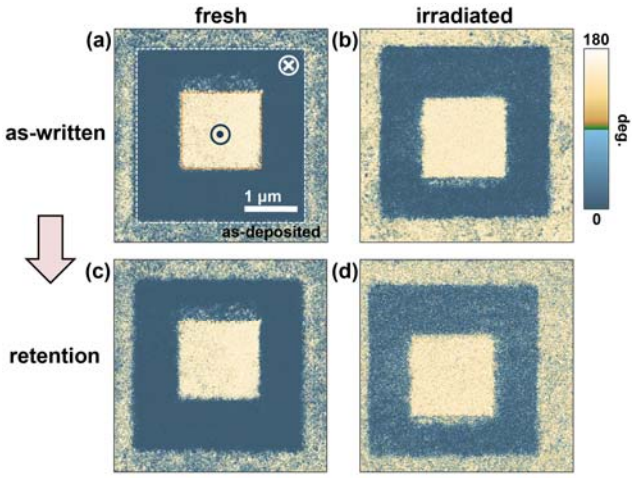
fresh
irradiated
(a)
(b)
as-written
1 μm
as-deposited
180
deg.
0
(c)
(d)
retention

FIG. 3

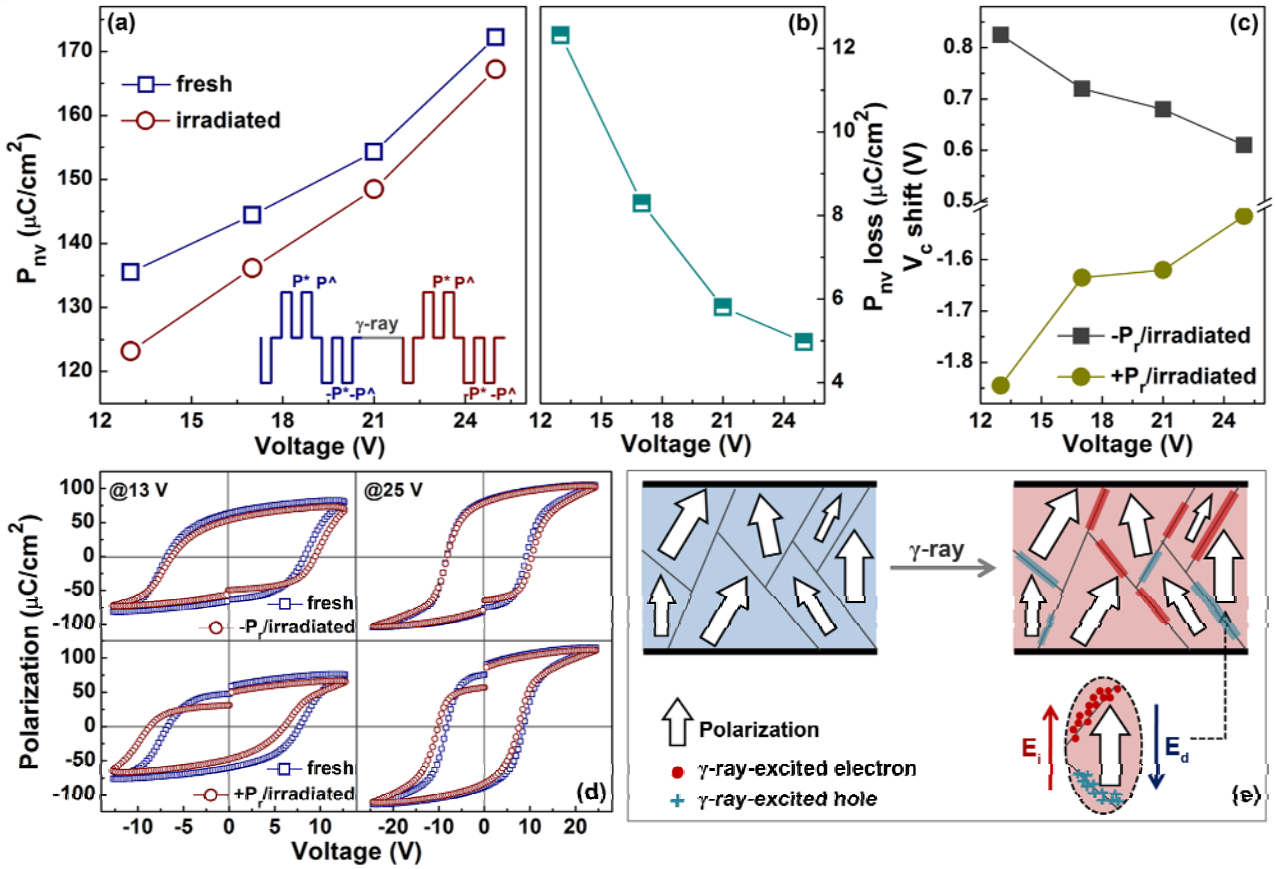
(a)
fresh
irradiated
P* P^
γ-ray
-P*-P^
P* P^
P* -P^
P_{nv} (μC/cm^2)
Voltage (V)
(b)
P_{nv} loss (μC/cm^2)
Voltage (V)
(c)
V_c shift (V)
-P_r/irradiated
+P_r/irradiated
Voltage (V)
@13 V
@25 V
fresh
-P_r/irradiated
fresh
+P_r/irradiated
(d)
Polarization (μC/cm^2)
Voltage (V)
γ-ray
Polarization
γ-ray-excited electron
γ-ray-excited hole
E_i
E_d
(e)

FIG. 4

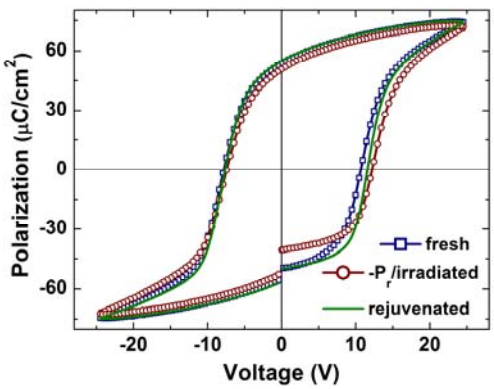
Polarization (μC/cm²)
60
30
0
-30
-60
-20
-10
0
10
20
Voltage (V)
fresh
-P r /irradiated
rejuvenated

FIG. 5

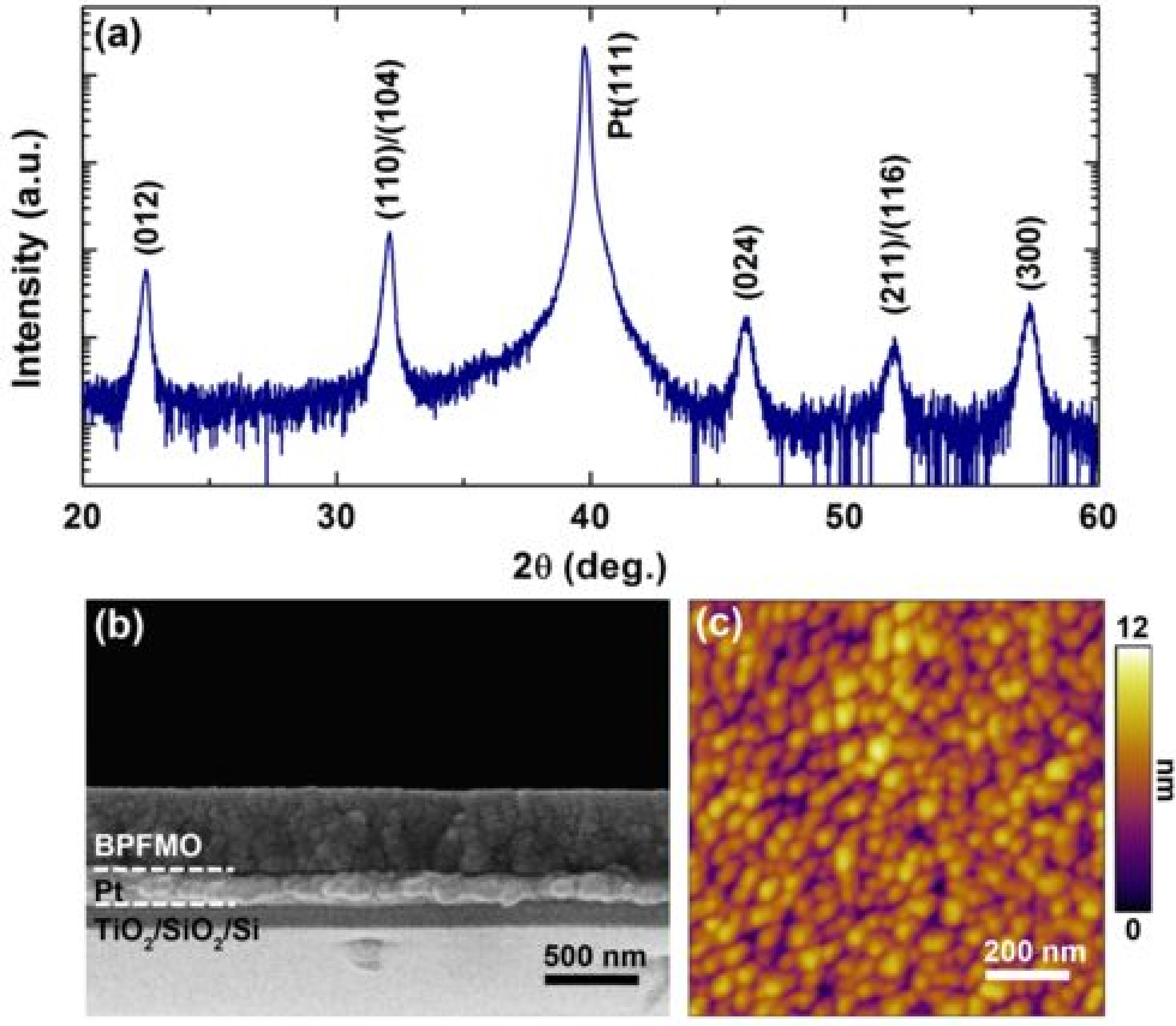
(a)
Intensity (a.u.)
(012)
(110)/(104)
Pt(111)
(024)
(211)/(116)
(300)
20
30
40
50
60
2θ (deg.)
(b)
BPFMO
Pt
TiO2/SiO2/Si
500 nm
(c)
12
0
nm
200 nm

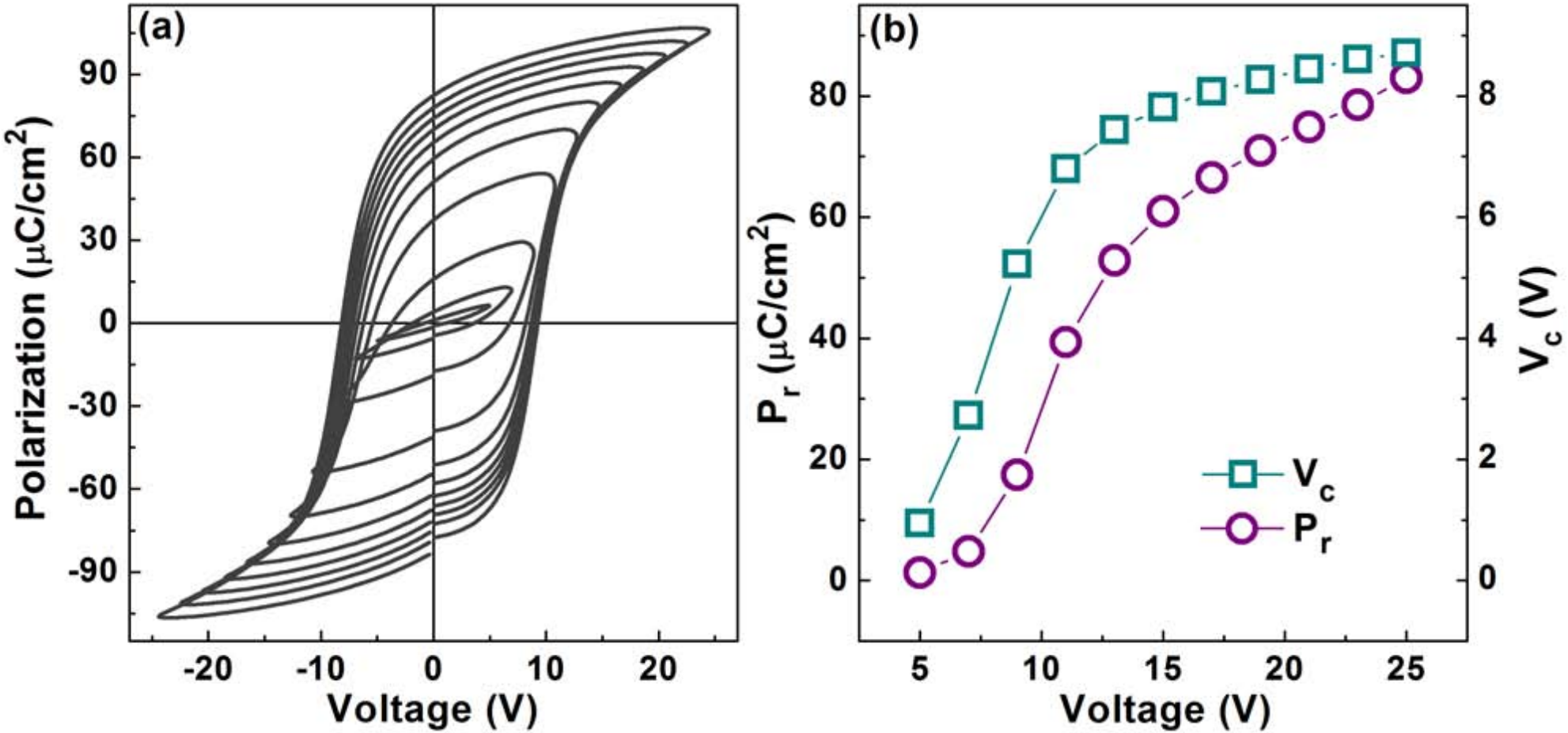
(a)
Polarization (μC/cm²)
90
60
30
0
-30
-60
-90
-20
-10
0
10
20
Voltage (V)
(b)
Pr (μC/cm²)
80
60
40
20
0
Vc (V)
8
6
4
2
0
5
10
15
20
25
Voltage (V)
Vc
Pr

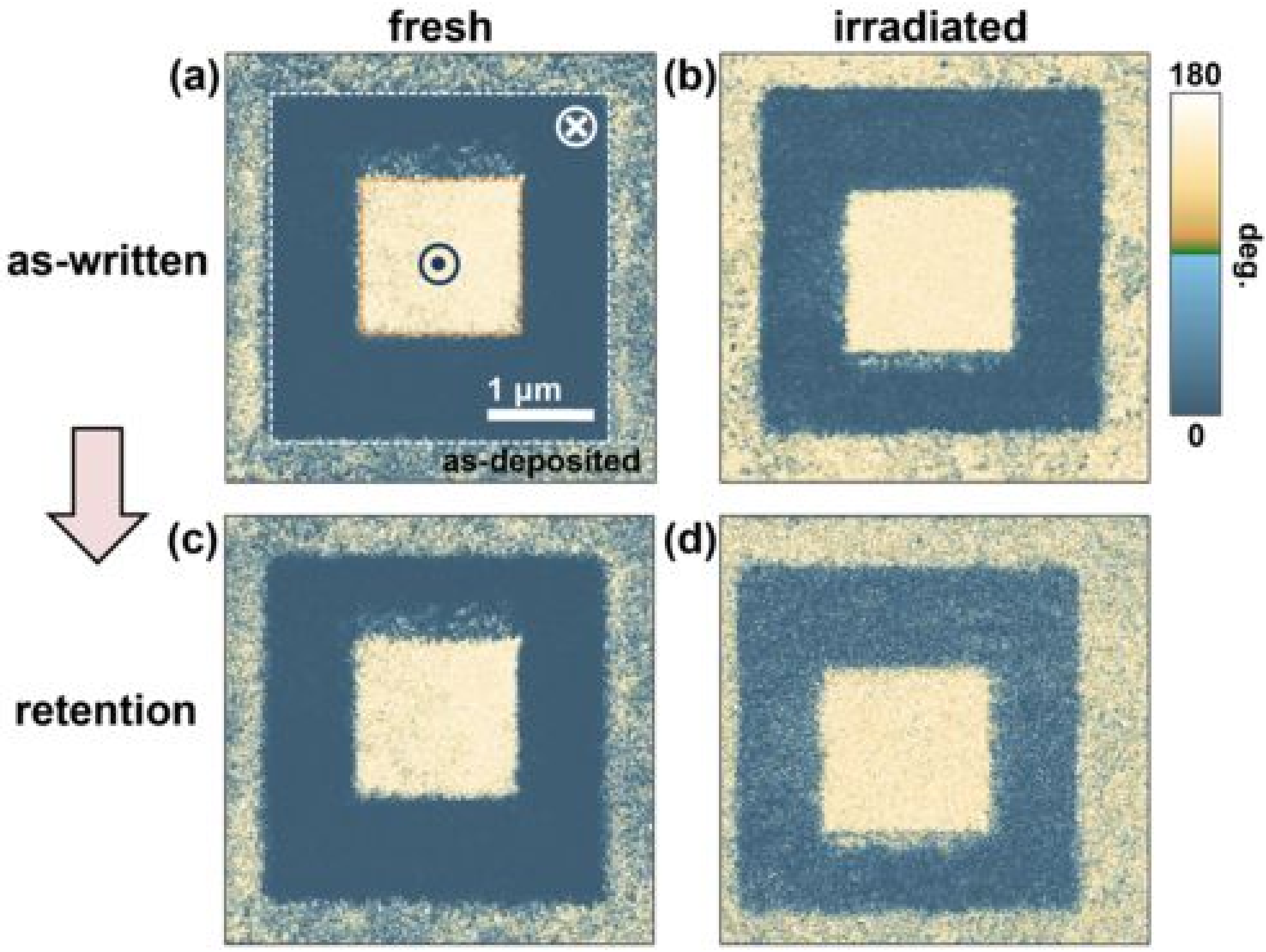
fresh
irradiated
(a)
(b)
as-written
1 μm
as-deposited
180
0
deg.
(c)
(d)
retention

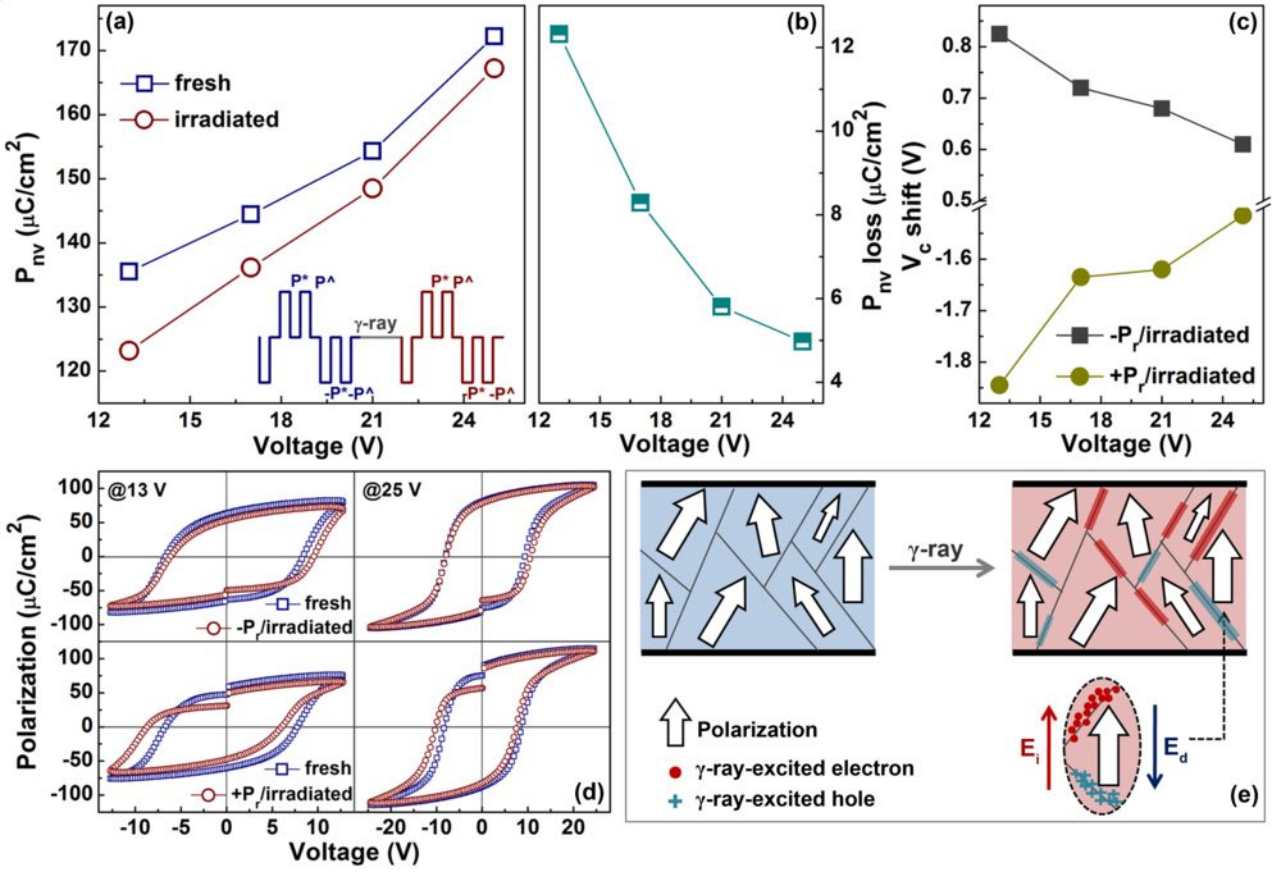
(a)
fresh
irradiated
P_{nv} (μC/cm^2)
Voltage (V)
P* P^
γ-ray
-P*-P^
P* P^
P* -P^
(b)
P_{nv} loss (μC/cm^2)
Voltage (V)
(c)
V_c shift (V)
-P_r/irradiated
+P_r/irradiated
Voltage (V)
@13 V
@25 V
fresh
-P_r/irradiated
fresh
+P_r/irradiated
Polarization (μC/cm^2)
Voltage (V)
(d)
γ-ray
Polarization
γ-ray-excited electron
γ-ray-excited hole
E_i
E_d
(e)

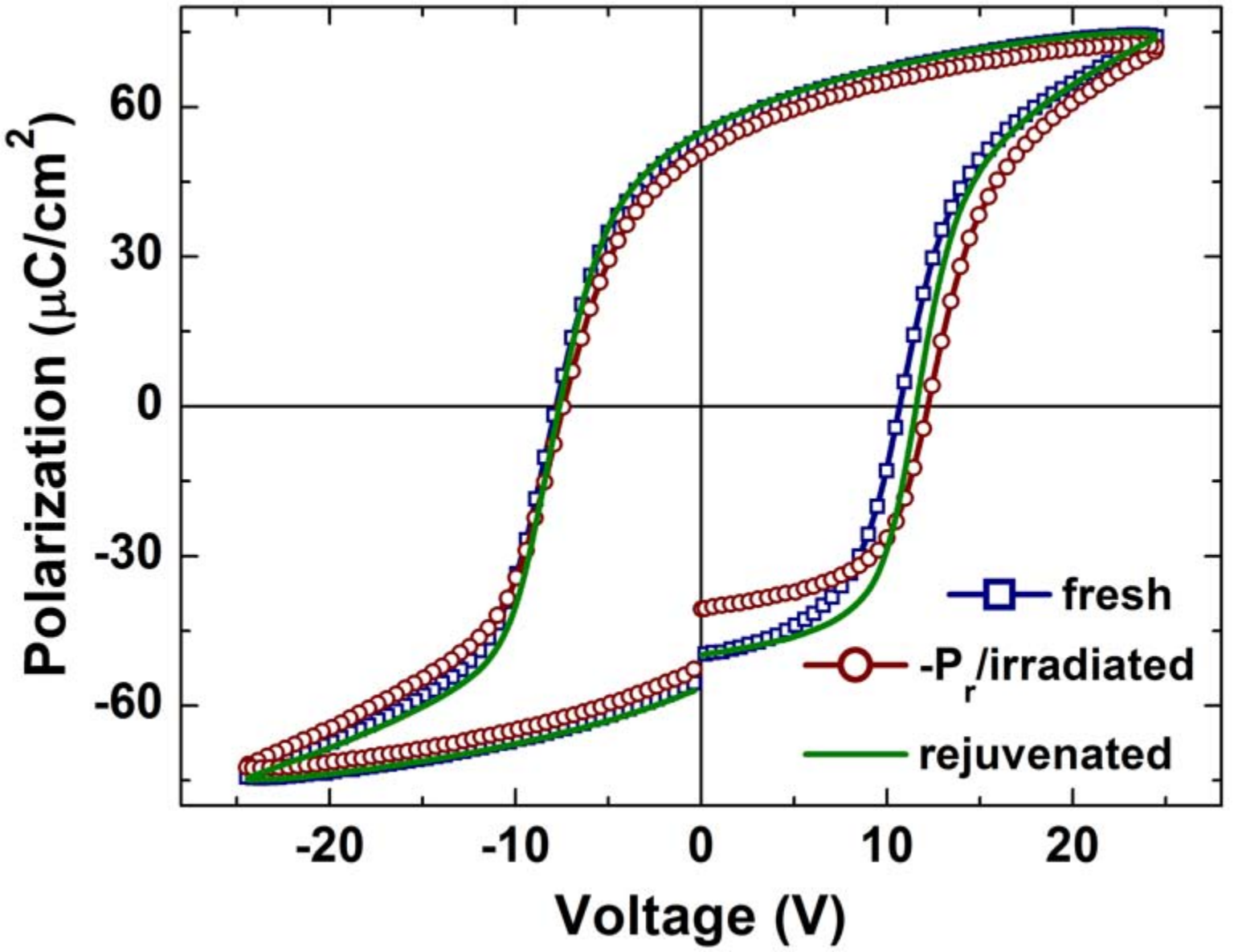
Polarization (μC/cm²)
60
30
0
-30
-60
-20
-10
0
10
20
Voltage (V)
fresh
-Pr/irradiated
rejuvenated